Theory and Gyro-fluid Simulations of Edge-Localized-Modes

BOUT++
Boundary Plasma Turbulence Code

X.Q.Xu[1], P.W.Xi[1,2], A.Dimits[1], I.Joseph[1], M.V.Umansky[1], T.Y.Xia[1,3], B.Gui[1,3], S.S.Kim[4], G.Y.Park[4], T.Rhee[4], H.Jhang[4], P.H.Diamond[4,5], B.Dudson[6], P.B.Snyder[7] ([1]LLNL,[2]PKU,[3]ASIPP,[4]NFRI,[5]UCSD,[6]U.York,[7]GA)

24th IAEA Fusion Energy Conference,

8-13 Oct. 2012,San Diego, USA

Principal Results

- **First order FLR corrections from "gyro-viscous cancellation" in two-fluid model are necessary to agree with gyro-fluid results for high ion temperature.**

- **Higher ion temperature introduces more FLR stabilizing effects, thus reduces ELM size.**

- **Developed a fast non-Fourier method for the computation of Landau-fluid closure terms;**
  - **Implemented the fast non-Fourier method through the solution of matrix equations in which the matrices are tridiagonal or narrowly banded;**

- **Implemented 3+0 {n, $u_{||}$, $P_{||}$} & 3+1 {{n, $u_{||}$, $P_{||}$},$P_{\perp}$} electrostatic model equations;**
- **Implemented 1+0 (n) & 2+0 {n, $u_{||}$} electromagnetic model for ELM simulations;**

- **Benchmarked linear GLF simulations with eigen-value calculations**
- **Benchmarked with other two-fluid codes;**

Table of Contents

- **Edge 3-field gyro-fluid models for type-I ELMs**

    - ✓ An isothermal electromagnetic 3-field gyro-fluid model with vorticity formulation generalized from Snyder-Hammett gyro-fluid model [1] for edge plasmas.
    - ✓ In long-wavelength limit, this set of gyro-fluid equations is reduced to previous 3-field two-fluid model with additional gyro-viscous terms resulting from the incomplete "gyro-viscous cancellation" in two-fluid model given by Xu et al [2].
    - ✓ Utilizing the Padé approximation for the modified Bessel functions, this set of gyro-fluid equations is implemented in the BOUT++ framework with full ion FLR effects.
    - ✓ An assumption of an ion steady-state with subsonic flow velocity leads to a model that the ion response is adiabatic for both equilibrium and axisymmetric component of fluctuations, such as $Z_i e<\Phi>=T_i \ln <P_i>$.

- **Edge 4-field gyro-fluid models for small ELMs**

- **A fast non-Fourier method for the computation of Landau-fluid closure terms**

- **BOUT++ core gyrofluid simulations of ion temperature gradient turbulence**

[1] P. B. Snyder and G. W. Hammett, Phys. Plasmas 8, 3199 (2001).
[2] X. Q. Xu, R. H. Cohen, T. D. Rognlien, et.al., Phys. Plasma 7, 1951 (2000).

3-field isothermal gyrofluid model* for ELM simulation: consider the large density gradient at H-mode pedestal

$$\frac{d\varpi_G}{dt} + \mathbf{V}_E \cdot \nabla \varpi_{G0} \boxed{- eB(\mathbf{V}_{\Phi T} - \mathbf{V}_{ET}) \cdot \nabla n_{iG}} = B\nabla_\parallel J_\parallel + 2\mathbf{b}_0 \times \mathbf{\kappa} \cdot \nabla \tilde{P}_G + \mu_{i,\parallel}\partial_\parallel^2 \varpi_G$$

$$\frac{d\tilde{P}_G}{dt} + \mathbf{V}_E \cdot \nabla P_{G0} \boxed{+ T_0(\mathbf{V}_{\Phi T} - \mathbf{V}_{ET}) \cdot \nabla n_{iG}} = 0$$

$$\frac{\partial A_\parallel}{\partial t} + \partial_\parallel \phi_T = \frac{\eta}{\mu_0}\nabla_\perp^2 A_\parallel - \frac{\eta_H}{\mu_0}\nabla_\perp^4 A_\parallel$$

$$\varpi_G = eB\left(\Gamma_0^{1/2}\tilde{n}_{iG} - n_0(1-\Gamma_0)\frac{e\phi}{T_0} + \frac{e\rho_i^2}{T_0}\nabla n_0 \cdot \nabla(\Gamma_0 - \Gamma_1)\phi - \tilde{n}_{iG}\right)$$

Padé approximation

$$\begin{cases}\Gamma_0^{1/2} \approx \dfrac{1}{1+b/2} \\[2mm] \Gamma_0 \approx \dfrac{1}{1+b} \\[2mm] \Gamma_0 - \Gamma_1 \approx 1\end{cases} \quad , \quad b = k_\perp \rho_i$$

$$d/dt = \partial/\partial t + \mathbf{V}_{ET} \cdot \nabla, \ \mathbf{V}_{ET} = \frac{1}{B}\mathbf{b}_0 \times \nabla\phi_T, \ \phi_T = \phi_0 + \phi, \ \nabla_\parallel f = B\partial_\parallel \frac{f}{B}, \ \partial_\parallel = \partial_\parallel^0 + \delta\mathbf{b}\cdot\nabla, \ \delta\mathbf{b} = \frac{1}{B}\nabla A_\parallel \times \mathbf{b}_0, \ J_\parallel = J_{\parallel 0} + \tilde{J}_\parallel, \ \tilde{J}_\parallel = -\nabla_\perp^2 A_\parallel / \mu_0$$

Twofluid equations

$$\frac{d\varpi}{dt} = B\nabla_\parallel J_\parallel + 2\mathbf{b}_0 \times \mathbf{\kappa} \cdot \nabla \tilde{P} + \mu_{i,\parallel}\partial_\parallel^2 \varpi$$

$$\frac{d\tilde{P}}{dt} + \mathbf{V}_E \cdot \nabla P_0 = 0$$

$$\frac{\partial A_\parallel}{\partial t} + \partial_\parallel \phi_T = \frac{\eta}{\mu_0}\nabla_\perp^2 A_\parallel - \frac{\eta_H}{\mu_0}\nabla_\perp^4 A_\parallel$$

$$\varpi = \frac{m_i n_0}{B}\left(\nabla_\perp^2 \phi + \frac{1}{en_0}\nabla_\perp^2 \tilde{P}_i + \frac{1}{n_0}\nabla n_0 \cdot \nabla\phi\right)$$

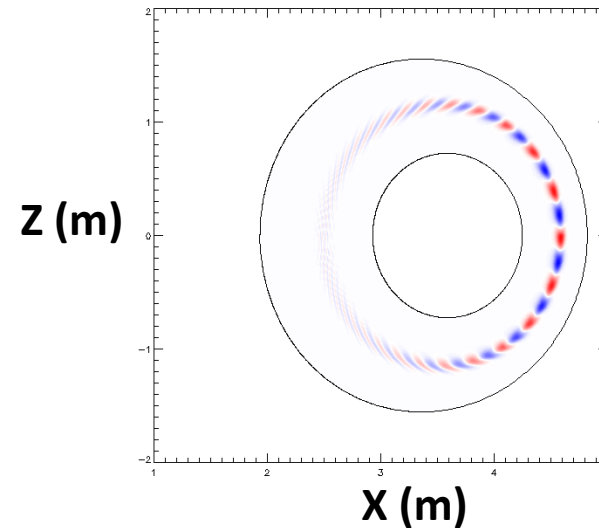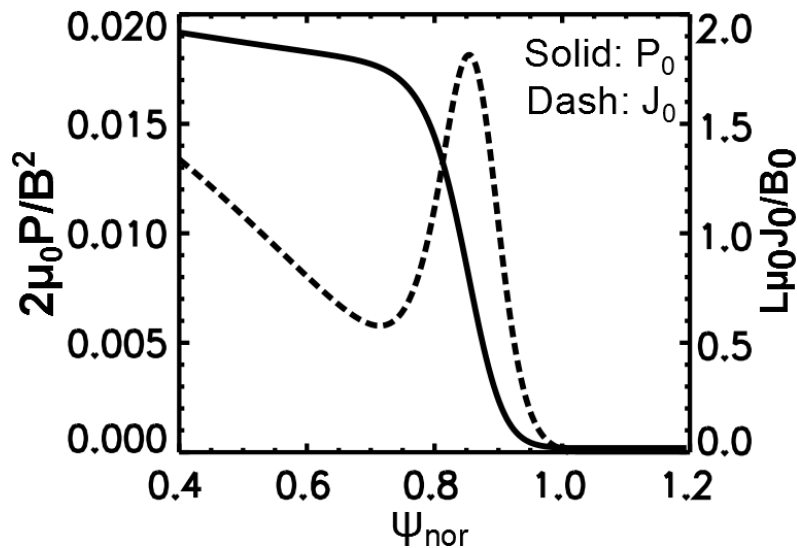**Relation between twofluid vorticity and gyrokinetic vorticity**

$$\varpi \approx \varpi_G + \frac{1}{2en_0}\nabla_\perp^2 \tilde{P}_{iG}$$

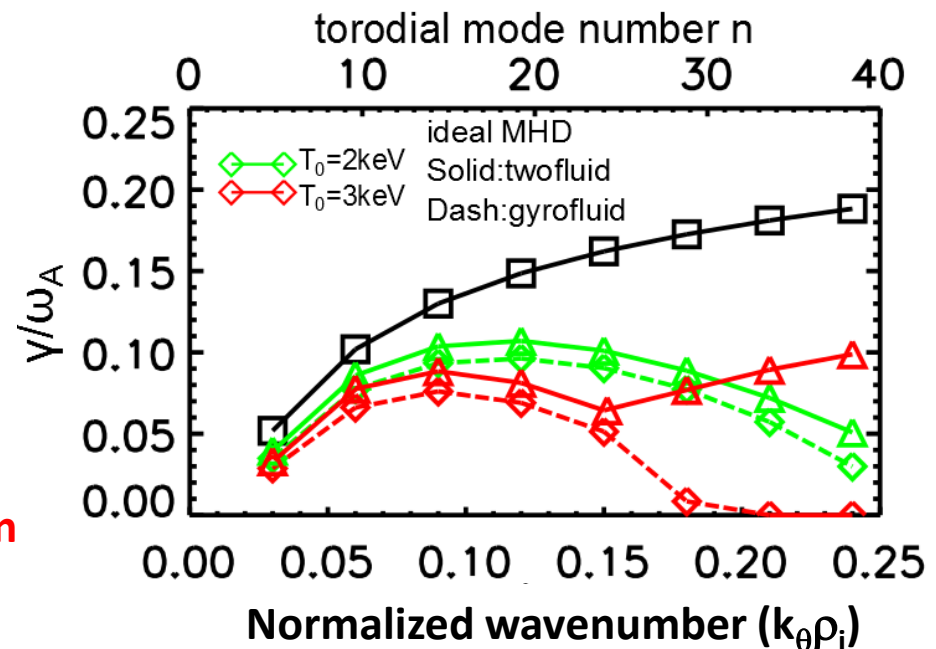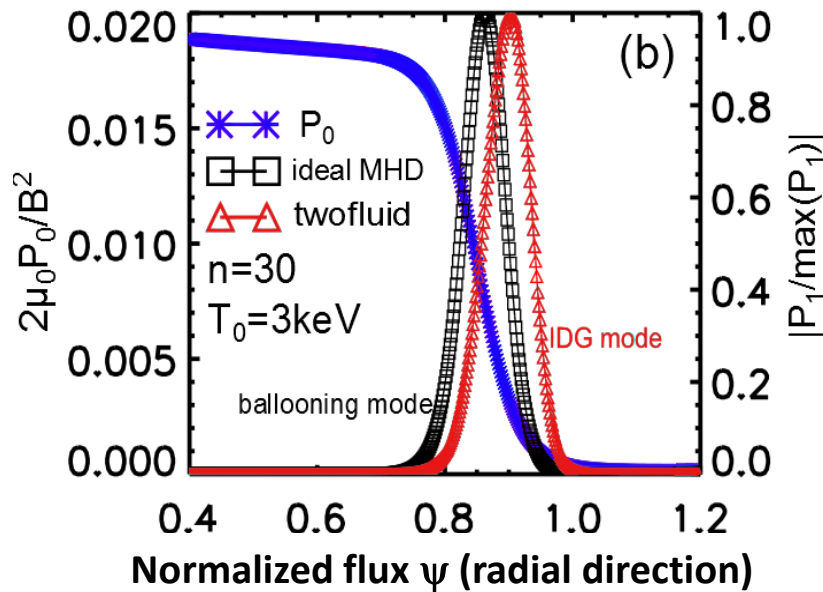*) P. B. Snyder and G. W. Hammett, *Phys. Plasmas* **8**, 3199 (2001)

Consider the **large density gradient** at H-mode pedestal:

➤ Two-fluid model: **no stabilizing** on high-n modes,

➤ Gyro-fluid model: **strong FLR stabilizing** on high-n modes.

What causes the disappear of stabilizing in twofluid model?

Ion-Density-Gradient mode in twofluid model

Normalized flux ψ (radial direction)

→ **The instability does not localize at peak pressure gradient region**
→ **Not pressure gradient driven ballooning mode, but other instability**
→ **Lowest order ballooning equation changes**

$$\frac{1}{J}\frac{\partial}{\partial\chi}\left[\frac{k_\perp^2}{B^2 J}\frac{\partial}{\partial\chi}\hat{\phi}\right] - \frac{\omega_J}{\rho_i^2 V_A}\left[\frac{i}{BJ}\frac{\partial}{\partial\chi}\hat{\phi}\right]$$
$$= -\left[\frac{k_\perp^2}{V_A^2}\omega(\omega + \omega_{*i} + i\frac{\omega}{k_\perp^2 n_0}\frac{dn_0}{d\psi}n\chi q' g^{\psi\psi}) + 2\frac{\omega_\kappa \omega_{*i}}{V_A^2 \rho_i^2}\right]\hat{\phi}$$

Twofluid local dispersion relation

| ion diamagnetic stabilizing on ballooning modes | drift instability due to ion density gradient |

$$\gamma = \frac{1}{\sqrt{C}}\left(\sqrt{\gamma_I^2 - \frac{\omega_{*i}^2}{4}}\cos\frac{\alpha}{2} + \frac{\omega_{*i}}{2}\sin\frac{\alpha}{2}\right)$$

$$C^2 = 1 + \frac{k_x^2}{k_\perp^4 L_n^2}, \quad \cos\alpha = \frac{1}{C}, \quad \sin\alpha = \frac{1}{C}\frac{k_x}{k_\perp^2 L_n}$$
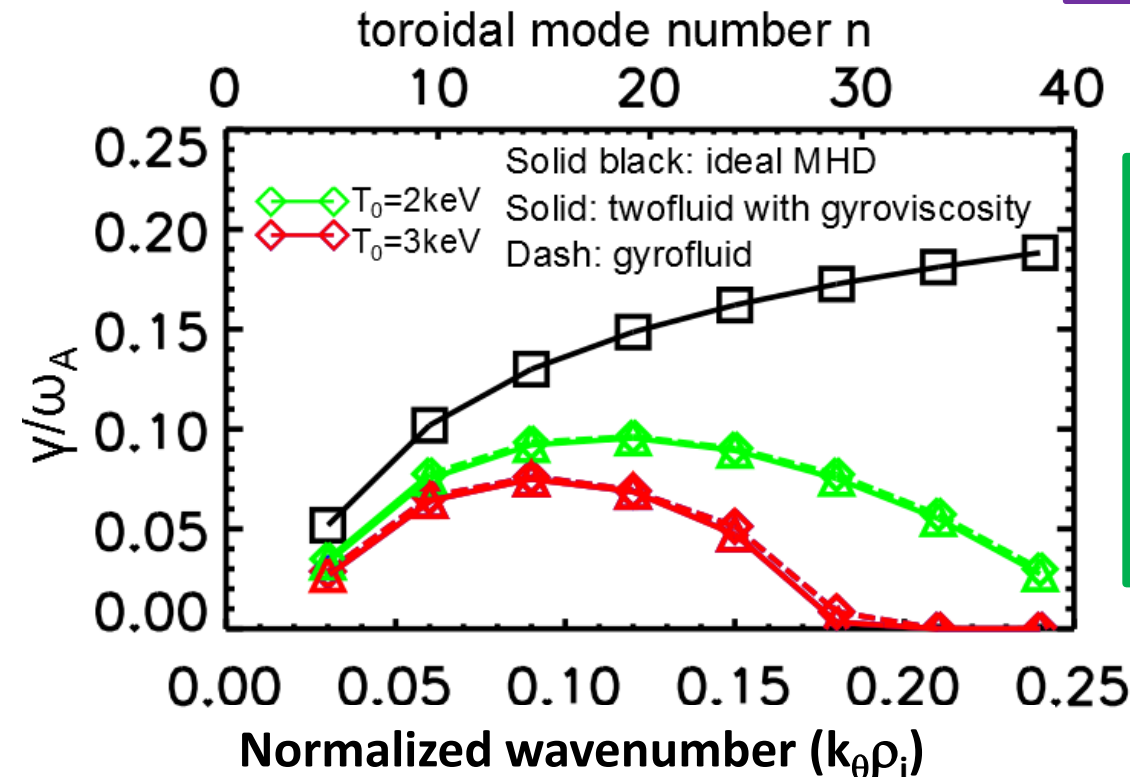
When ω_{*i} increases:

☐ Ion diamagnetic effect stabilizes ballooning modes → first term decreases
☐ Ion density gradient introduces
Ion-Density-Gradient mode: second term become dominant

Gyroviscous terms are necessary to stabilize Ion-Density-Gradient modes and should be kept in twofluid model

Only ion diamagnetic effect in two-fluid model is not sufficient to represent FLR stabilizing if density gradient is large!

- At long wavelength limit, gyro-fluid goes back to two-fluid but with additional **gyroviscous terms**

$$\frac{d\varpi_G}{dt} + \mathbf{V} \cdot \nabla \varpi_{G0} - eB(\mathbf{V}_{\Phi T} - \mathbf{V}_{ET}) \cdot \nabla n_{iG} = \frac{d\varpi}{dt} + \frac{1}{2\omega_{ci}} \left\{ \nabla_\perp^2 [\phi, P_i] - [\nabla_\perp^2 \phi, P_i] - [\phi, \nabla_\perp^2 P_i] \right\}$$

toroidal mode number n

Solid black: ideal MHD
Solid: twofluid with gyroviscosity
Dash: gyrofluid

$T_0 = 2$keV
$T_0 = 3$keV

γ/ω_A

Normalized wavenumber ($k_\theta \rho_i$)

- **Gyroviscous terms [1] represent necessary FLR effect to stabilize IDG modes and should be kept in twofluid model**
- **If without gyroviscous terms, IDG mode will lead to much larger ELM crash in nonlinear phase**

[1] X. Q. Xu, R. H. Cohen, T. D. Rognlien, et.al., Phys. Plasma 7, 1951 (2000).
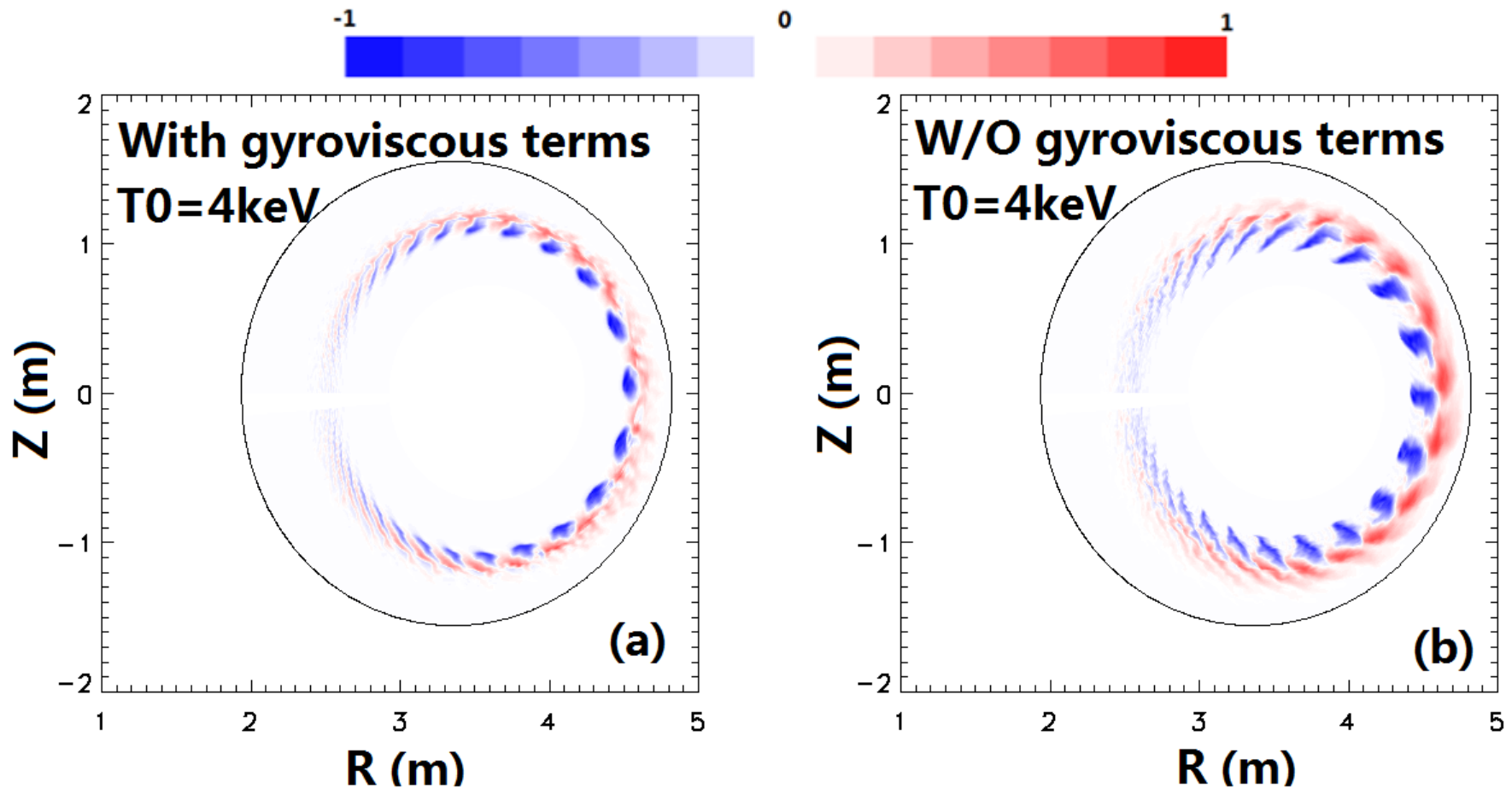
Pressure perturbation at ELM crash time

ELM size: 0.06   **ELM size: 0.13**

In isothermal limit, linear relation for n=0 component of electric field cannot get nonlinear saturation
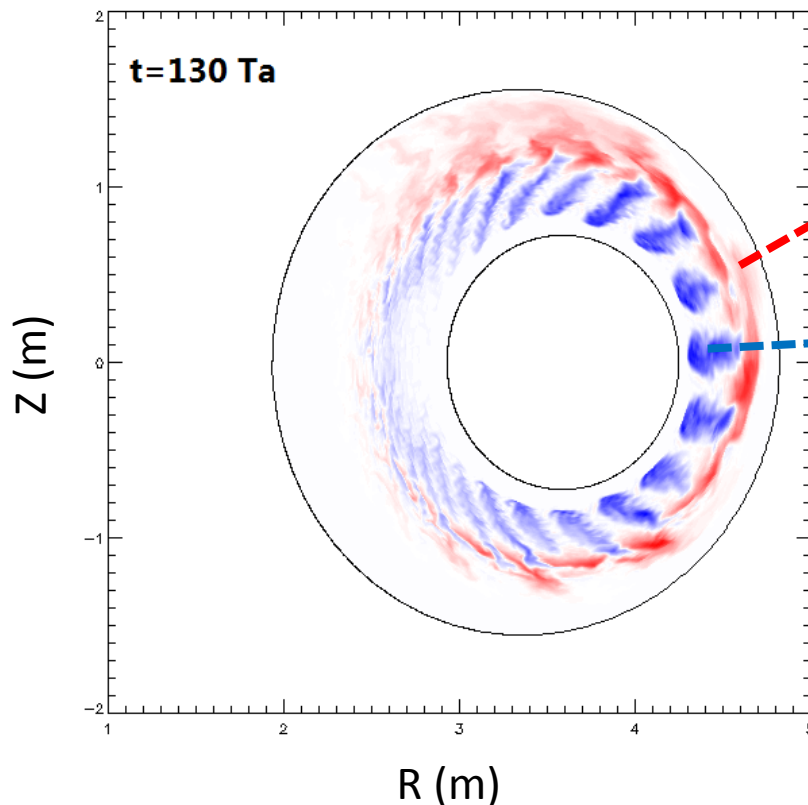
Net zonal flow is set to be zero:

$$\langle \varpi_T \rangle = 0$$

Equilibrium part:

$$\langle \varpi_0 \rangle = 0 \Rightarrow \phi_0 = -\frac{T_0}{e} \ln P_{i0}$$

Linear relation:

$$\langle \varpi \rangle = \frac{n_{i0} m_i}{B} (\nabla_\perp^2 \phi_{dc} + \frac{1}{n_{i0}} \nabla n_{i0} \cdot \nabla \phi_{dc} + \frac{1}{n_{i0} e} \nabla_\perp^2 \tilde{P}_{i,dc}) = 0 \Rightarrow linear \quad \phi_{dc}$$

t=130 Ta

Z (m)

R (m)

Strong n=0 **EXB:**
➢ Smooth perturbation in poloidal direction
➢ Reduce radial transport

Very weak n=0 **EXB:**
➢ Keep streamer like structure
➢ Cannot reduce radial transport
➢ No saturation

✓ **n=0 component of electric field determines the saturation phase;**
✓ **This linear relation is not correct.**

Nonlinear relation generates larger EXB shearing at pedestal top to get the saturation phase
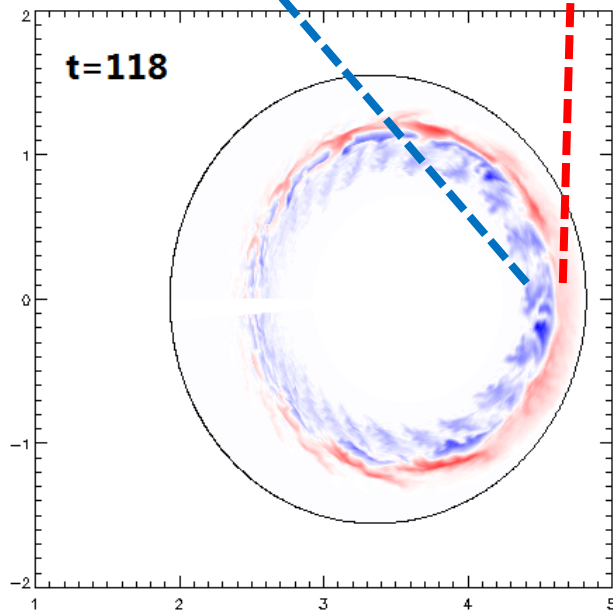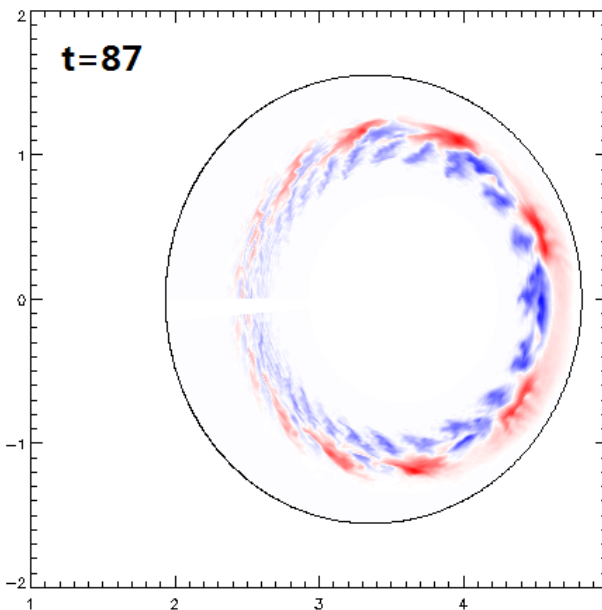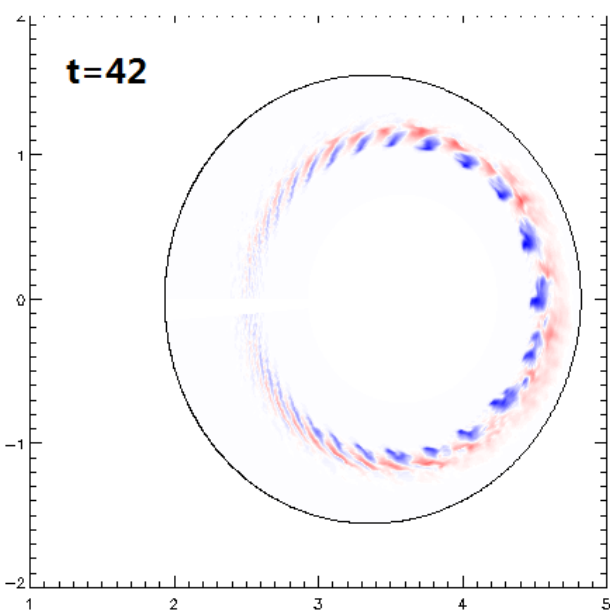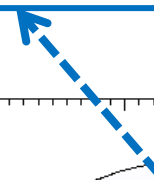

twofluid
T=5keV

t=0
t=42
t=87
t=118
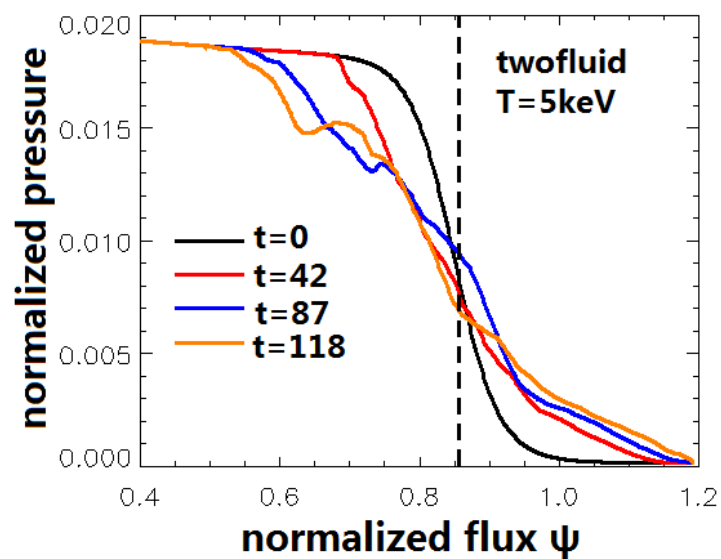
$$\langle \varpi_T \rangle = \frac{n_{i0}m_i}{B}\left(\nabla_\perp^2(\phi_{dc}+\phi_0) + \frac{1}{n_{i0}}\nabla n_{i0}\cdot\nabla(\phi_{dc}+\phi_0) + \frac{1}{n_{i0}e}\nabla_\perp^2(\tilde{P}_{i,dc}+P_{i0}) \right) = 0$$

$$\Rightarrow \phi_{dc} = -\frac{T_0}{e}\ln\left(\frac{\tilde{P}_{i,dc}+P_{i0}}{P_{i0}} \right) \quad \text{(nonlinear relation)}$$
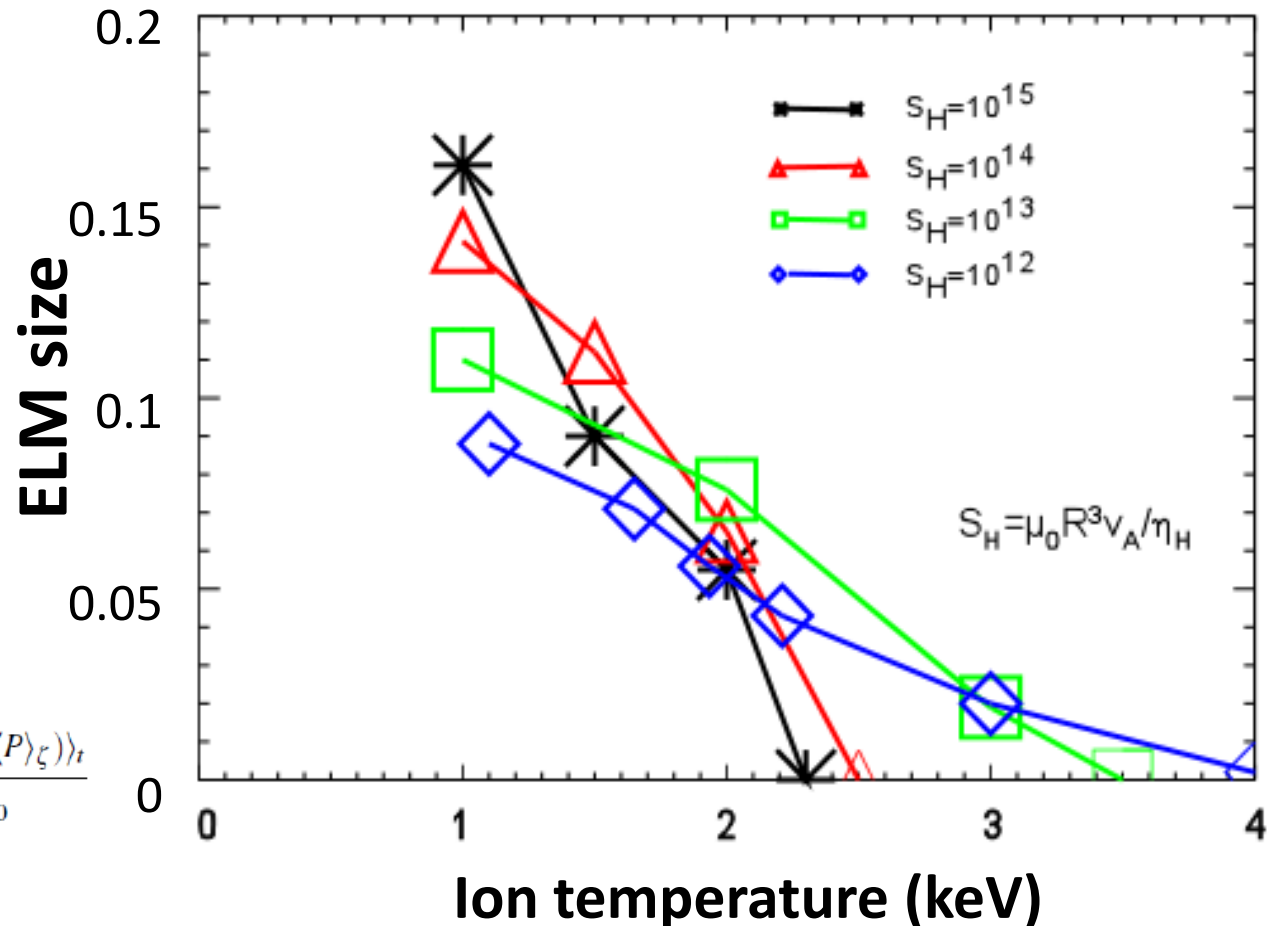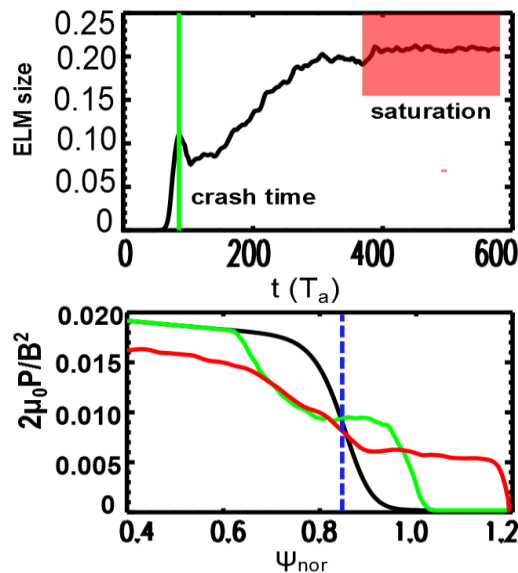
Pedestal bottom: n=0 EXB is still strong due to 1/n0

Pedestal top: n=0 EXB flow is enough to reduce radial transport and generate saturation

t=42

t=87

t=118

Higher ion temperature introduces more FLR stabilizing effects, thus reduces ELM size

- Hyper-resistivity is necessary to ELM crash, but ELM size is weakly sensitive to hyper-resistivity;
- With fixed pressure profile, high ion temperature introduce stronger FLR effect and thus leads to smaller ELM size
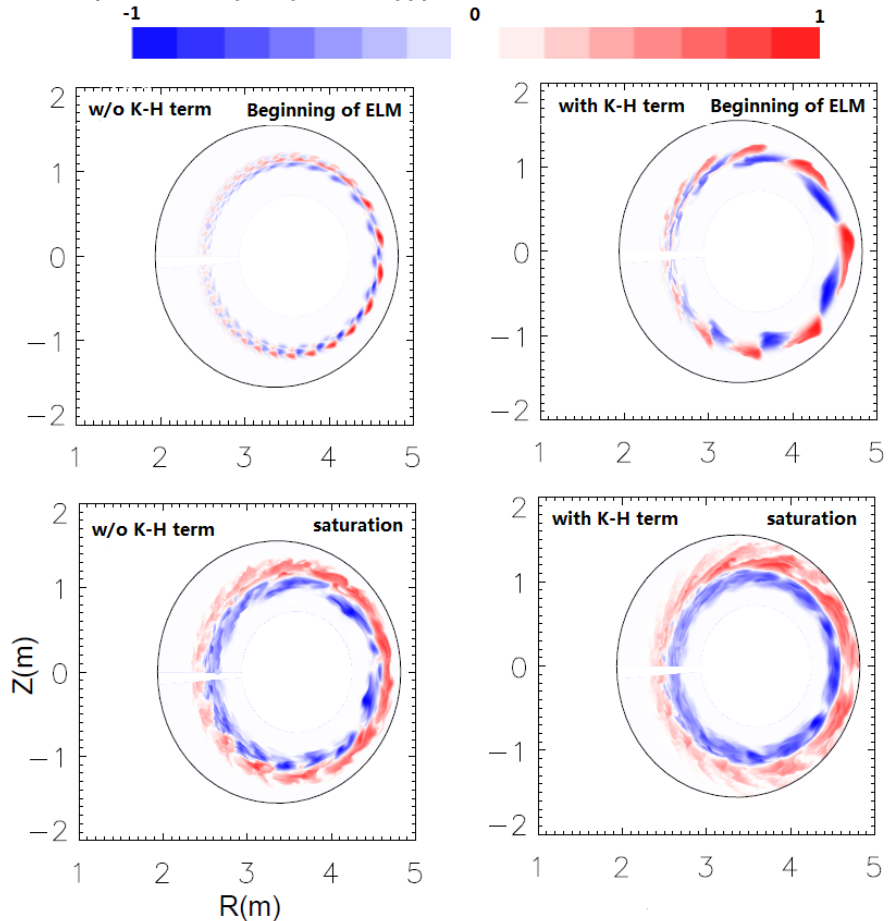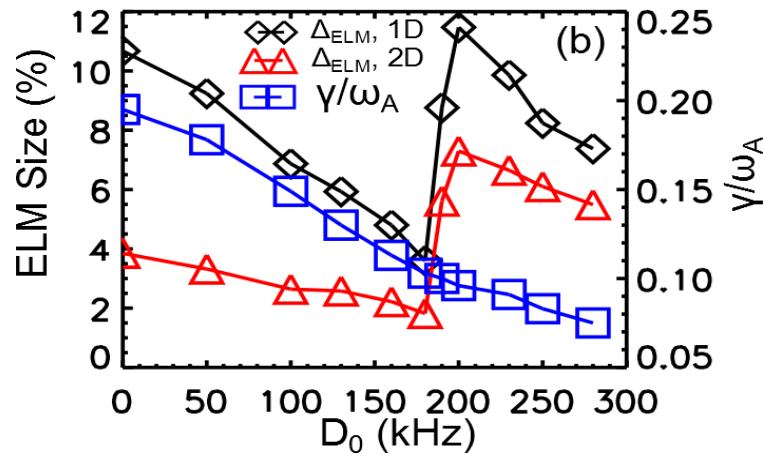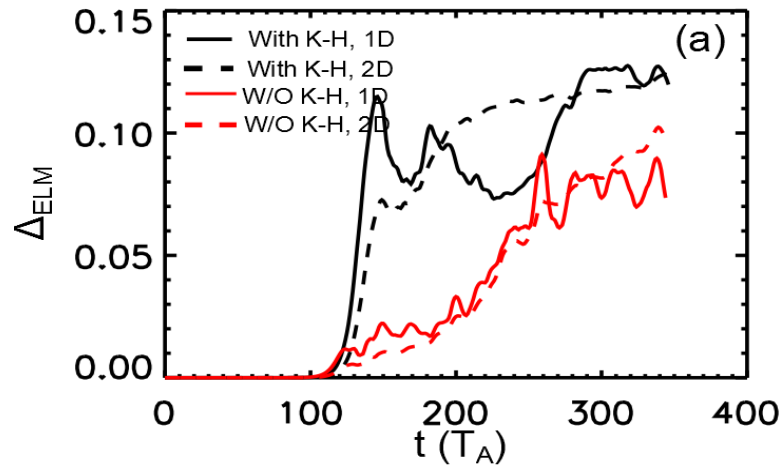

$$\Delta_{ELM}^{th} = \frac{\Delta W_{ped}}{W_{ped}} = \frac{\langle \int_{R_{in}}^{R_{out}} \oint dR d\theta (P_0 - \langle P \rangle_\zeta) \rangle_t}{\int_{R_{in}}^{R_{out}} \oint dR d\theta P_0}$$

$S_H = 10^{15}$
$S_H = 10^{14}$
$S_H = 10^{13}$
$S_H = 10^{12}$

$S_H = \mu_0 R^3 v_A / \eta_H$

ELM size

Ion temperature (keV)

(Without density gradient in vorticity)

Equilibrium EXB shear flow can stabilize high-n ballooning modes and reduce ELM size, but introduces Kelvin-Helmholtz instability and leads to larger ELM when flow shear is too large.

$$\frac{\partial \varpi}{\partial t} + \mathbf{V}_{E \times B} \cdot \nabla \varpi + \boxed{\mathbf{V}_1 \cdot \nabla \varpi_0} = B_0 \nabla_\parallel J_\parallel + 2\mathbf{b}_0 \times \kappa \cdot \nabla P$$

$$\mathbf{V}_{E \times B} = \frac{\mathbf{b} \times \nabla \Phi_{dia0}}{B} + \frac{\mathbf{b} \times \nabla \Phi_{V0}}{B} + \frac{\mathbf{b} \times \nabla \phi}{B}$$

$$\Phi_{dia0} = -\frac{P_{i0}}{Zen_{i0}}, \qquad \frac{d\Phi_{V0}(\psi)}{d\psi} = D_0[1 - \tanh(D_s(x - x_0))] + C$$

P. W. Xi, X. Q. Xu, X. G. Wang, and T. Y. Xia, *Phys. Plasmas* **19**, 092503 (2012)

2+0 isothermal gyrofluid model for ELM simulation

Gyrokinetic Vorticity

$$\frac{d\varpi_G}{dt} - eB(\mathbf{V}_\Phi - \mathbf{V}_E) \cdot \nabla n_{iG} = B\nabla_\parallel J_\parallel + 2\mathbf{b}_0 \times \kappa \cdot \nabla \tilde{P} - B\nabla_\parallel en_0(\bar{u}_{\parallel i} - \tilde{u}_{\parallel i}) + eB(\bar{\nabla}_\parallel - \nabla_\parallel)n_0\tilde{u}_{\parallel i}$$

Pressure

$$\frac{dP_G}{dt} + T_i(\mathbf{V}_\Phi - \mathbf{V}_E) \cdot \nabla n_{iG} + \nabla_\parallel P_0\tilde{u}_{\parallel i} - \frac{T_0}{e}\nabla_\parallel J_\parallel + \nabla_\parallel \frac{P_0}{2}(\bar{u}_{\parallel i} - \tilde{u}_{\parallel i}) + (\bar{\nabla}_\parallel - \nabla_\parallel)\frac{P_0\tilde{u}_{\parallel i}}{2} = 0$$

Ion parallel momentum

$$m_in_0\frac{d\tilde{u}_{\parallel i}}{dt} + m_in_0(\mathbf{V}_\Phi - \mathbf{V}_E) \cdot \nabla \tilde{u}_{\parallel i} + \partial_\parallel P_G + en_0\frac{\partial(\bar{A}_\parallel - A_\parallel)}{\partial t} + (\bar{\partial}_\parallel - \partial_\parallel)\tilde{p}_i + (\delta\bar{\mathbf{b}} - \delta\mathbf{b}) \cdot \nabla \frac{P_0}{2} = 0$$

Ohm's law

$$\frac{\partial A_\parallel}{\partial t} + \partial_\parallel \phi - \frac{1}{n_0e}\partial_\parallel P_e = \eta J_\parallel + \eta_H \nabla_\perp^2 \tilde{J}$$
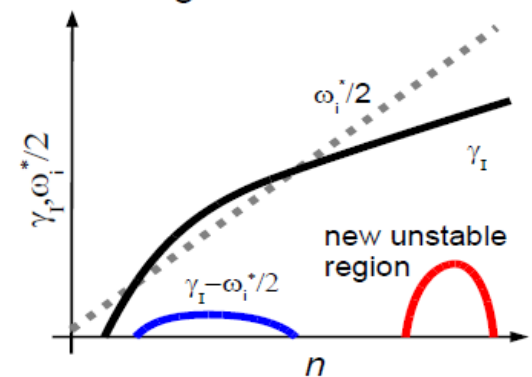
Vorticity definition

$$\varpi_G = eB(\Gamma_0^{1/2}\tilde{n}_{iG} - n_0(1 - \Gamma_0)\frac{e\phi}{T_0} + \frac{e\rho_i^2}{T_0}\nabla n_0 \cdot \nabla((\Gamma_0 - \Gamma_1)\phi) - \tilde{n}_{iG})$$

where $d/dt = \partial/\partial t + \mathbf{V}_E \cdot \nabla$, $\mathbf{v}_E = \frac{1}{B}\mathbf{b}_0 \times \nabla \phi$, $\mathbf{V}_\Phi = \frac{1}{B}\mathbf{b} \times \nabla \Phi = \frac{1}{B}\mathbf{b} \times \nabla \Gamma_0^{1/2}\phi$, $J_\parallel = J_0 + \tilde{J}_\parallel$, $J_{0\parallel} = -en_{0e}u_{0\parallel e}$, $\bar{u}_i = \Gamma_0^{1/2}\tilde{u}_{\parallel i}$ $\delta\mathbf{b} = \frac{1}{B}\nabla A_\parallel \times \mathbf{b}$, $\delta\bar{\mathbf{b}} = \frac{1}{B}\nabla \bar{A}_\parallel \times \mathbf{b}$, $\bar{A}_\parallel = \Gamma_0^{1/2}A_\parallel$, $\nabla_\parallel f = B\partial_\parallel \frac{f}{B}$, $\partial_\parallel = \partial_\parallel^0 + \delta\mathbf{b} \cdot \nabla$

- Including ion acoustic wave
  → drift ballooning modes*
  → May appear at high-n region → **gyrofluid**

Schematic view of kinetic effects on IBM growth rate

*R. J. Hastie et al. *Phys. Plasma* **10**(2003) 4405

Aiba, 2011, H-mode workshop

➢Ion parallel motion ⟶ ion acoustic wave
➢Electron pressure in Ohm's law ⟶ electron drift wave

$$\omega_{*i} = -\omega_{*e} = \frac{1}{2Bn_0e}\mathbf{b}\times\nabla P_0\cdot\mathbf{k}_\perp$$

$$\omega_s = c_s/Rq$$

Local dispersion relation*

$$-\omega(\omega-\omega_{*i})\left[(1+2q^2)\omega_s^2-\omega(\omega-\omega_{*e})\right] = \gamma_I^2\left[\omega_s^2-\omega(\omega-\omega_{*e})\right]$$
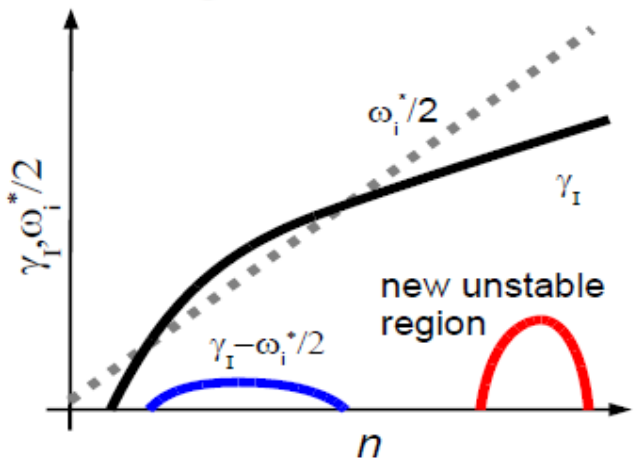
Wave resonance condition

$$f_{res} = |(1+2q^2)\omega_s^2-\omega_{*i}(\omega_{*i}-\omega_{*e})|$$

Ion diamagnetic stabilizing disappear

$$f_{res} = 0 \rightarrow wave\ resonance$$

Implied from local theory

Our results

Schematic view of kinetic effects on IBM growth rate

$\gamma_I, \omega_i^*/2$

$\omega_i^*/2$

γ_I

$\gamma_I-\omega_i^*/2$

new unstable region

n

Ideal MHD
GF
GF+P_e+V_i

γ/ω_A

n
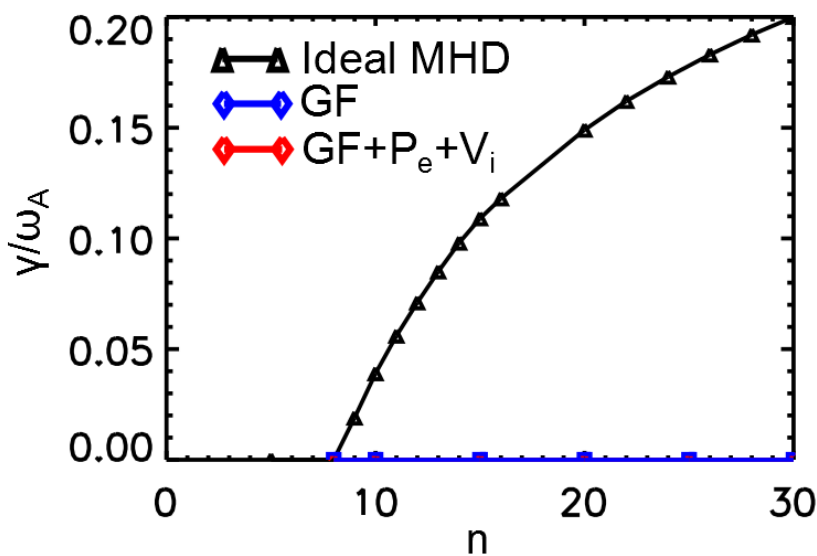
*R. J. Hastie et al. *Phys. Plasma* **10**(2003) 4405

NO drift ballooning mode!

14

Local dispersion relation*

$$- \omega(\omega - \omega_{*i}) \left[(1 + 2q^2)\omega_s^2 - \omega(\omega - \omega_{*e}) \right] = \gamma_I^2 \left[\omega_s^2 - \omega(\omega - \omega_{*e}) \right]$$

$$\delta\omega = \omega - \omega_{*i}$$
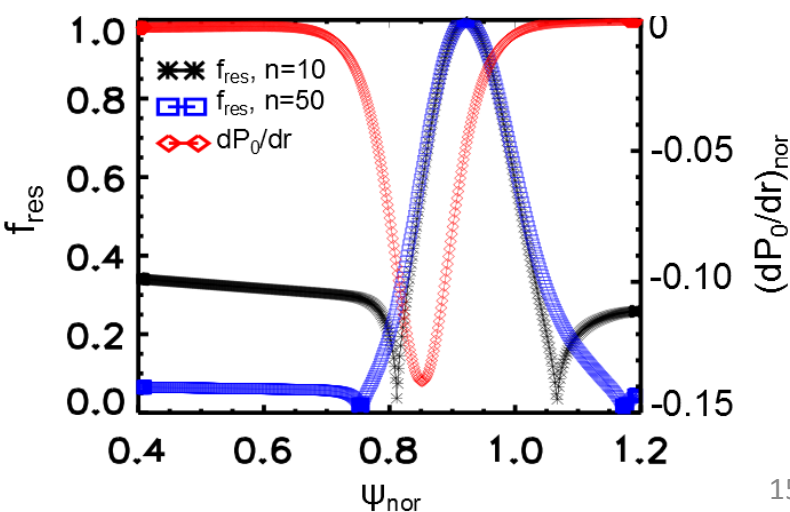$$\Delta\omega^2 = (1 + 2q^2)\omega_s^2 - \omega_{*i}(\omega_{*i} - \omega_{*e})$$

$$\omega_{*i} \sim \omega_{*e} \sim \omega_s$$
$$\frac{\delta\omega}{\omega_{*i}} \sim \frac{|\Delta\omega^2|}{\omega_{*i}^2} \sim \frac{\gamma_I}{\omega_{*i}} \sim \epsilon \ll 1$$

$$\gamma \propto \sqrt{(\omega_{*i}\Delta\omega^2)^2 - 8q^2(1 + 2q^2)\omega_{*i}(2\omega_{*i} - \omega_{*e})\omega_s^2\gamma_I^2}$$

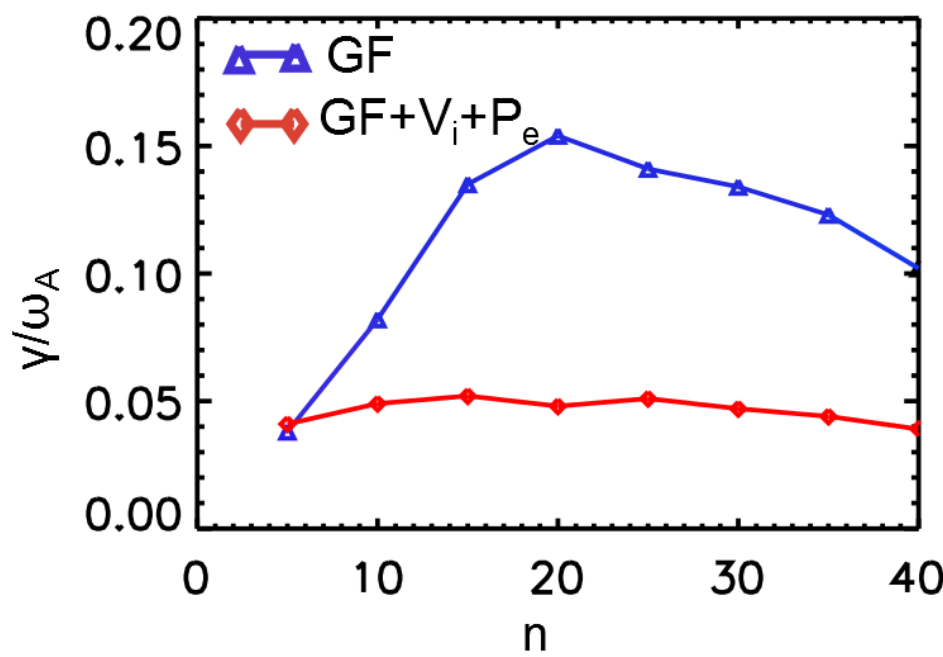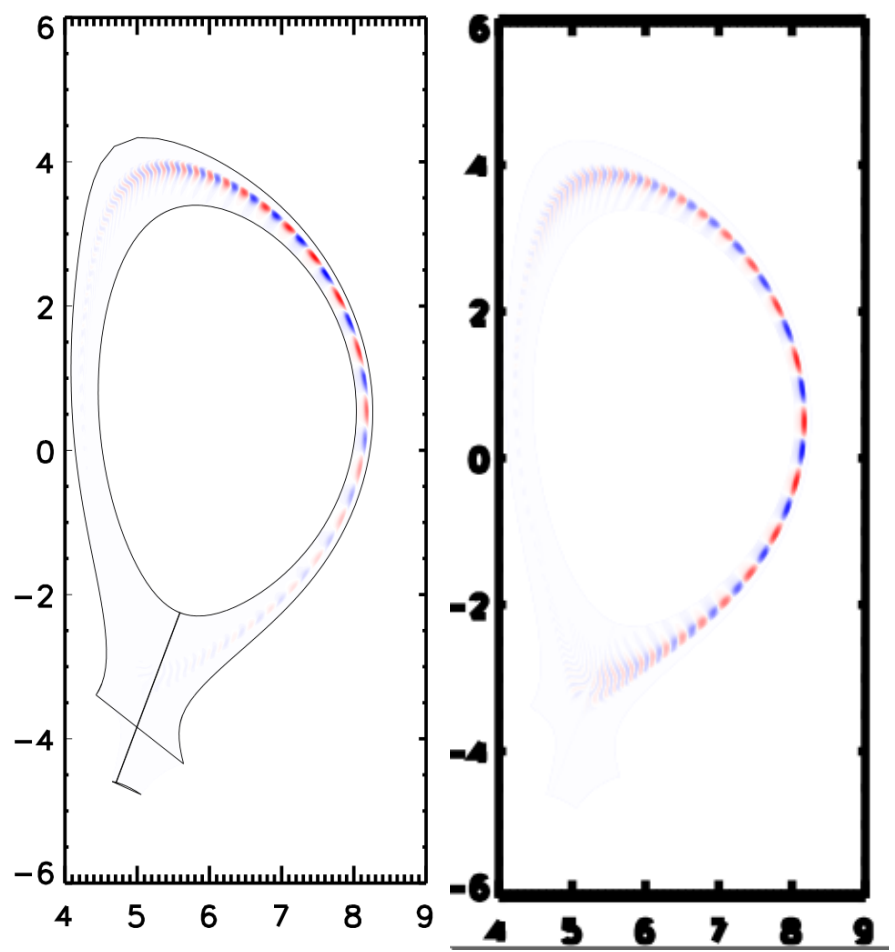- **Conditions for drift ballooning**

  A: Finite local **i**deal MHD growth rate
  B: Wave resonant condition is satisfied at the finite pressure gradient region

  n=10 → **B** not **A**
  n=50 → **A** not **B**

In real discharges, these two conditions are difficult to satisfy simultaneously.

$$f_{res} = |(1 + 2q^2)\omega_s^2 - \omega_{*i}(\omega_{*i} - \omega_{*e})|$$
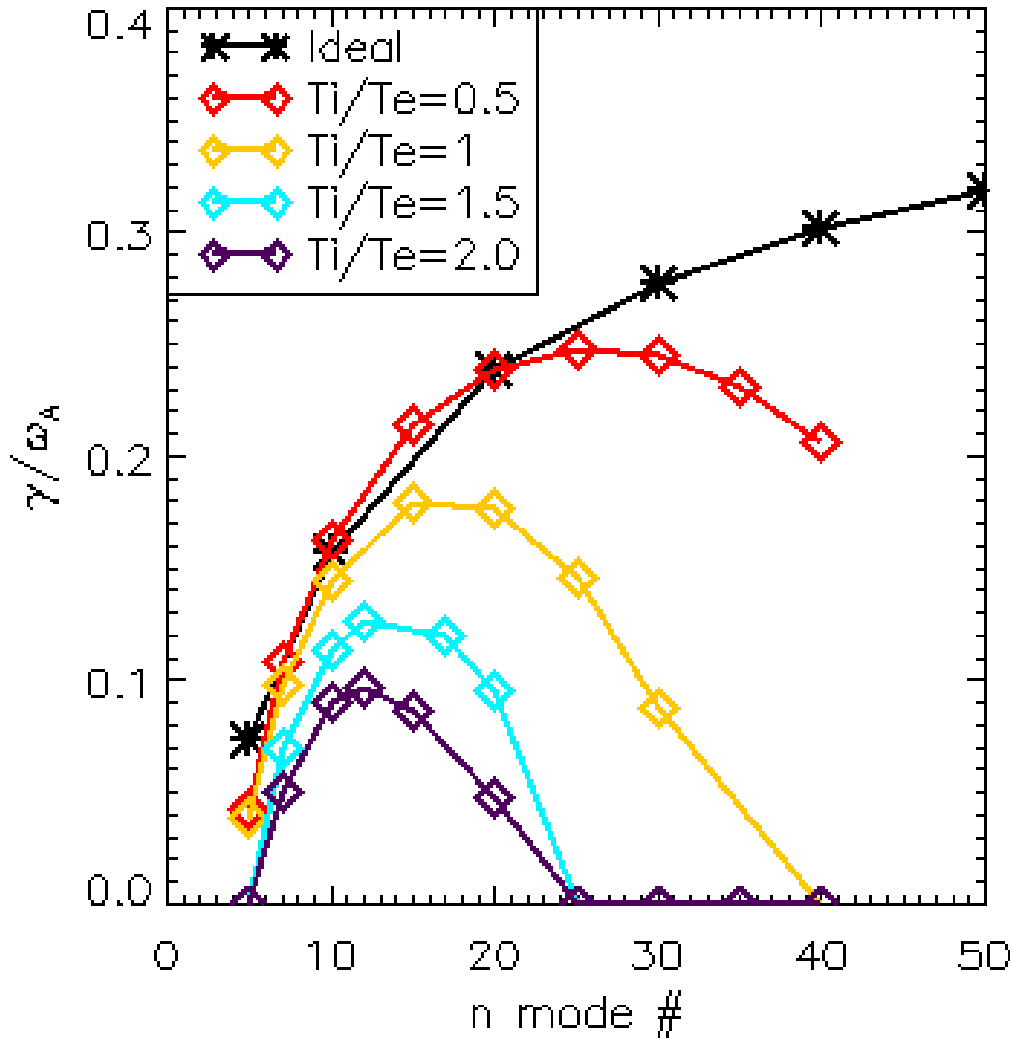
W/O Vi/Pe   **With Vi/Pe**

ITER

Ion acoustic wave and electron drift wave has stabilizing effect on P-B mode

Drift ballooning mode is unlikely the instability triggering small ELM in real discharges (DIIID, C-Mod, NXTX, ITER)

16

T. N. Rhee, et al

Equation set of 4 field model (normalized)

Beta originated from compressibility

Rest terms

$$\frac{\partial P}{\partial t} = -\vec{V}_E \cdot \nabla P + \frac{\beta}{1 + \beta / 2B_0^2}\left[-B_0\nabla_\parallel\left(\frac{V_\parallel}{B_0} + 2\delta J\right) - 2\vec{b}_0\times\vec{\kappa}_0\cdot\left(\nabla\varphi - \frac{\delta_e}{B_0}\nabla P\right)\right],$$

$$\frac{\partial V_\parallel}{\partial t} = -\vec{V}_E \cdot \nabla V_\parallel - \frac{1}{2}\nabla_\parallel P,$$

$$\frac{\partial U}{\partial t} = -\vec{V}_E \cdot \nabla U - B_0^2\nabla_\parallel J + \vec{b}_0\times\vec{\kappa}_0\cdot\nabla P + \frac{\delta_i}{2B_0}\left[\vec{V}_E\cdot\nabla(\nabla_\perp^2 P) - \nabla_\perp^2(\vec{V}_E\cdot\nabla P) - V_D\cdot\nabla(\nabla_\perp^2\varphi)\right],$$

Additional FLR effects

$$\frac{\partial\psi}{\partial t} = -\frac{\nabla_\parallel(B_0\varphi)}{B_0} + \frac{\delta_e}{B_0}\nabla_\parallel P + \frac{1}{S}\nabla_\perp^2\psi - \frac{1}{S_H}\nabla_\perp^4\psi, \ S = \mu_0\overline{L}V_A/\eta, \ S_H = \mu_0\overline{L}^3V_A/\eta_H$$

where B_0 is normalized variable

$$\delta = \frac{1}{2\Omega\overline{T}}, \ \Omega = \frac{e\overline{B}}{m_i}, \ \tau = T_i/T_e, \ \delta_i = \frac{\tau}{1+\tau}\delta, \ \delta_e = \frac{1}{1+\tau}\delta, \ \beta = \frac{2\mu_0 P_0}{\overline{B}^2},$$

$$J = \nabla_\perp^2\psi, \ A_\parallel = B_0\psi, \ \Phi = B_0\varphi, \ d/dt = \partial/\partial t + V_E\cdot\nabla, \ \nabla_\parallel = \partial_\parallel^0 - b\times\nabla\psi\cdot\nabla,$$

$$\vec{V}_E = b_0\times\nabla\varphi, \ \vec{V}_D = b_0\times\nabla P, \ U = \nabla_\perp^2\varphi + \frac{\delta_i}{B_0}\nabla_\perp^2 P$$

Vorticity with diamagnetic effect

Accurate non-Fourier methods for Landau-fluid operators

Tokamak edge:

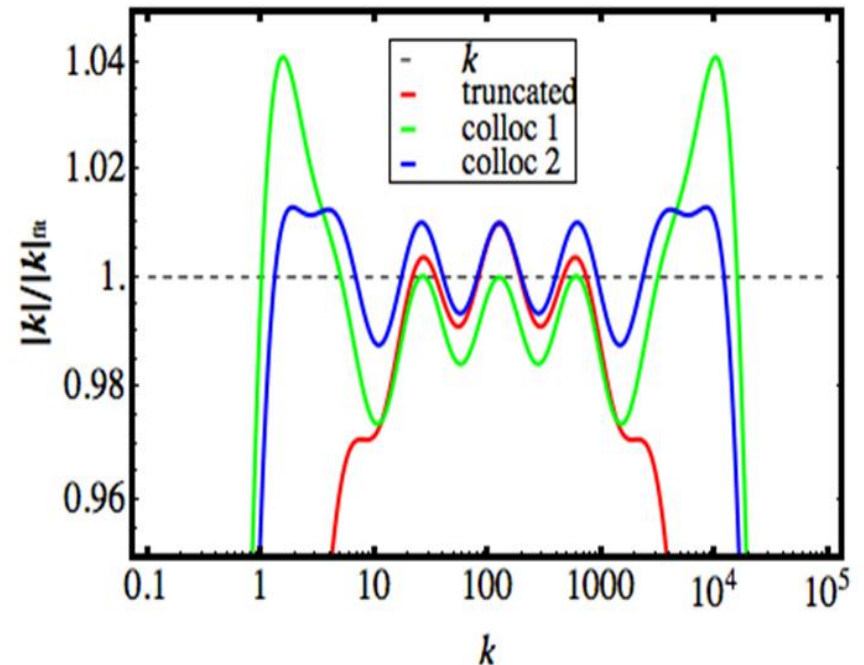- **kinetic effects important -> need Landau-fluid (LF) operators**

$$\gamma \propto -v_{\text{char}} \left| k \right|$$

- **Large spatial inhomogeneities & complicated boundary**
  - **need non-Fourier implementation**
  - **Useful accurate approximation:**

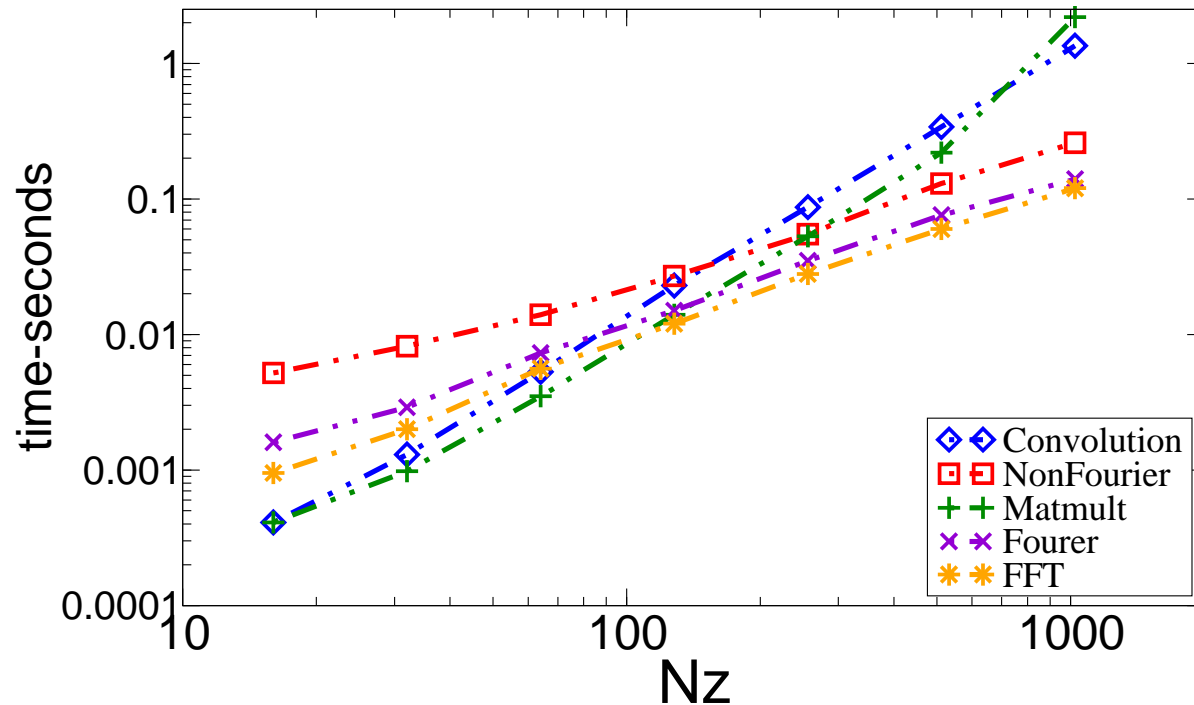$$\frac{1}{|k|} \approx \sum_{n=0}^{N} \frac{\alpha^n k_0}{k^2 + \left(\alpha^n k_0\right)^2}$$

- **The new method has Fourier-like computational scaling**

Ratio of fit to analytical operator vs. wavenumber

✓ **The error is less than 1.5%.**

- For small number of grid cells, direct matrix multiplication is as efficient as Fourier

- Non-Fourier, with fixed N, scales as N_z, c.f. N_z^2 for direct convolution

- Crossover point is at $N_z \approx 100 - 200 \Rightarrow$ advantage for $N_z \geq 100 - 200$.

$$\frac{\partial}{\partial t}n + \frac{\partial}{\partial z}(un) = 0$$

$$\frac{\partial}{\partial t}(mnu) + \frac{\partial}{\partial z}(umnu) = -\frac{\partial}{\partial z}p + enE - \frac{\partial}{\partial z}S$$

$$\frac{\partial}{\partial t}p + \frac{\partial}{\partial z}(up) = -(\Gamma-1)(p+S)\frac{\partial}{\partial z}u - \frac{\partial}{\partial z}q$$

$$q_k = -n_0\chi_1 \frac{\sqrt{2}V_t}{|k|}ikT_k$$

$$S_k = -mn_0\mu_1 \frac{\sqrt{2}V_t}{|k|}iku_k$$

$$\chi_1 = 2/\sqrt{\pi}$$

$$\mu_1 = 0$$

$$\Gamma = 3$$

$$\frac{1}{|k|} \approx \beta\sum_{n=0}^{N}\frac{\alpha^n}{k^2+\alpha^{2n}}$$

$$q_k = \sum_{n=0}^{N}q_k^n = -\chi_1\sqrt{2}\left(\beta\sum_{n=0}^{N}\frac{\alpha^n}{k^2+\alpha^{2n}}\right)ikT_k$$

$$q_k^n = -\chi_1\sqrt{2}\beta\frac{\alpha^n}{k^2+\alpha^{2n}}ikT_k$$

$$\left(k^2+\alpha^{2n}\right)q_k^n = \left(-\chi_1\sqrt{2}\beta\alpha^n\right)ikT_k$$

$$\left(-\frac{\partial^2}{\partial z^2}+\alpha^{2n}\right)q^n(z) = \left(-\chi_1\sqrt{2}\beta\alpha^n\right)\frac{\partial}{\partial z}T(z)$$

Response function

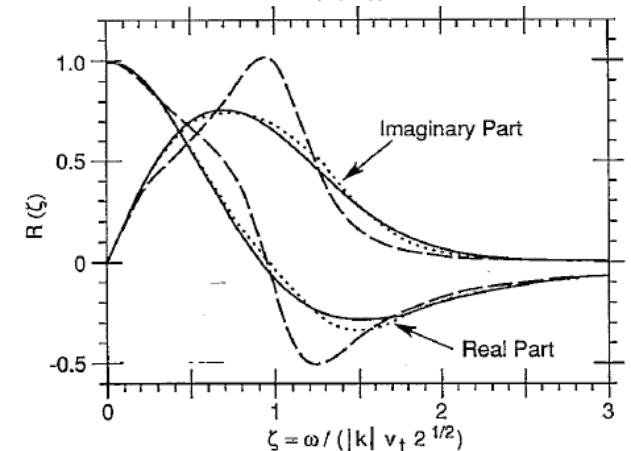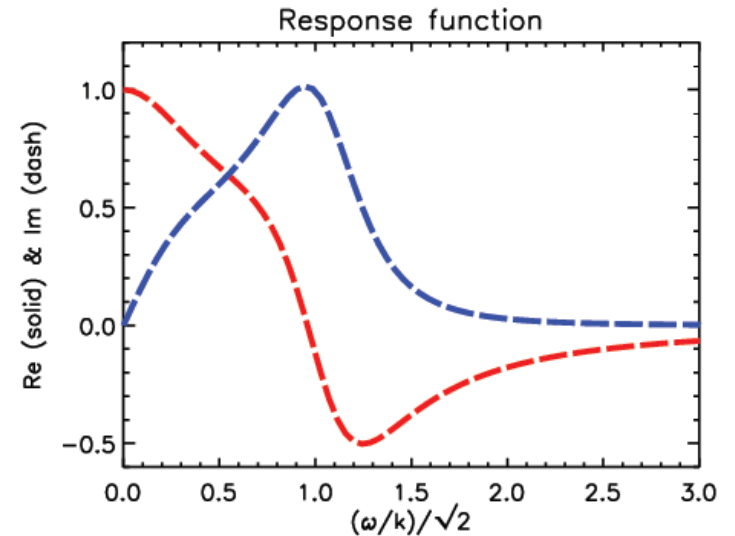
FIG. 1. The real and imaginary parts of the normalized response function $R(\zeta) = -\bar{n}T_0/n_0e\bar{\phi}$ vs the normalized frequency ζ. The solid lines are the exact kinetic result for a Maxwellian, $R(\zeta) = 1 + \zeta Z(\zeta)$. The dashed lines are from the three-moment fluid model with $\Gamma=3$, $\mu_1=0$, and $\chi_1=2/\sqrt{\pi}$. The dotted lines are from the four-moment model.

Nonlocal closure for q(T) uses sum of Lorentzians

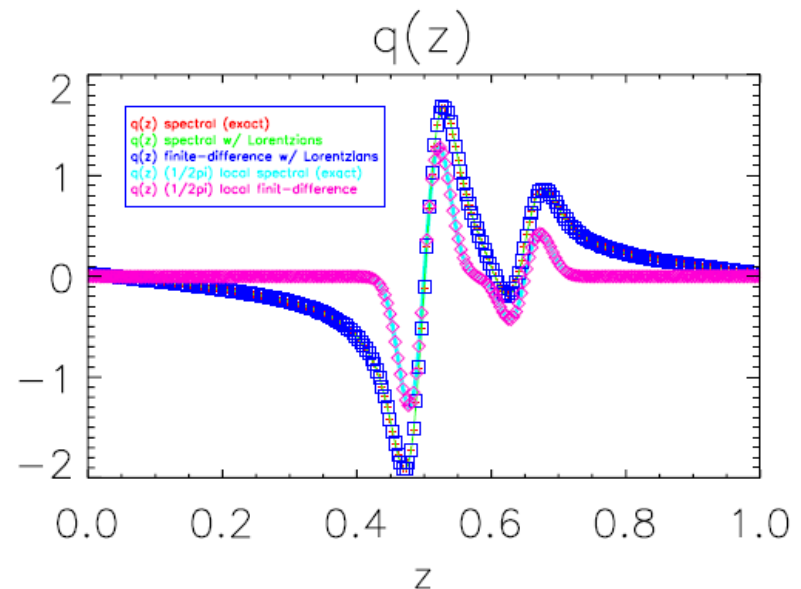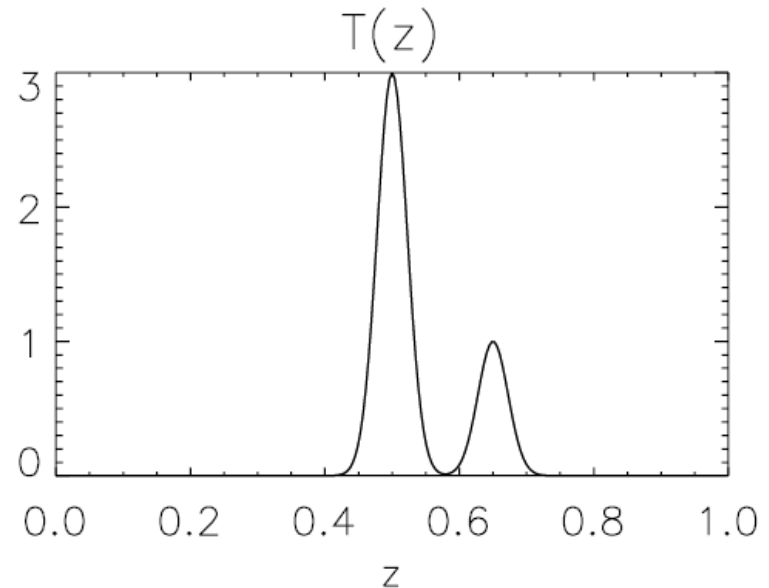**Representation of sign(k) by sum of Lorentzians is used; leads to 2nd order ODE**

$$q(z) = \sum q_n(z)$$

$$\left(A_n \frac{\partial^2}{\partial z^2} + B_n\right) q_n = \frac{\partial}{\partial z} T(z)$$

Using B.C. q=0 at z_{min}, z_{max}

Tested in stand-alone IDL code:

1) **Spectral exact**
2) **Spectral with Lorentzians**
3) **Finite-difference with Lorentzians**

T(z)

q(z)

q(z) spectral (exact)
q(z) spectral w/ Lorentzians
q(z) finite-difference w/ Lorentzians
q(z) (1/2pi) local spectral (exact)
q(z) (1/2pi) local finit-difference
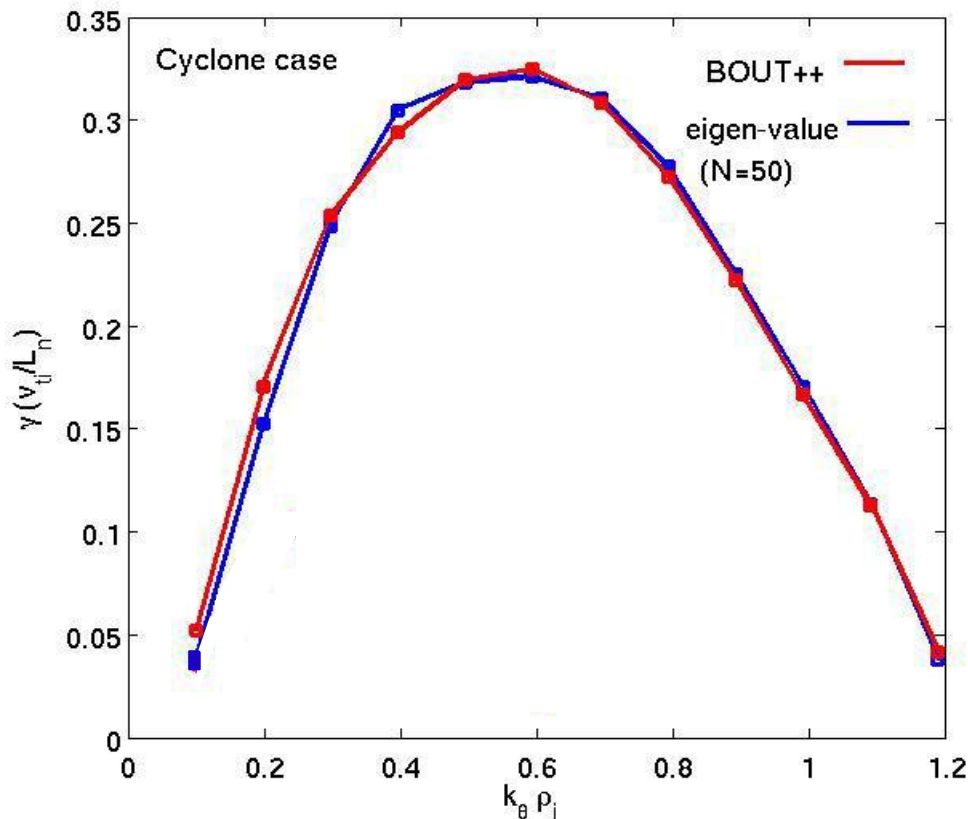
BOUT++ gyro-fluid results approach gyro-kinetic results

The fluid moment approach generates an approximation to the kinetic equation that increases in accuracy as more moments are retained.
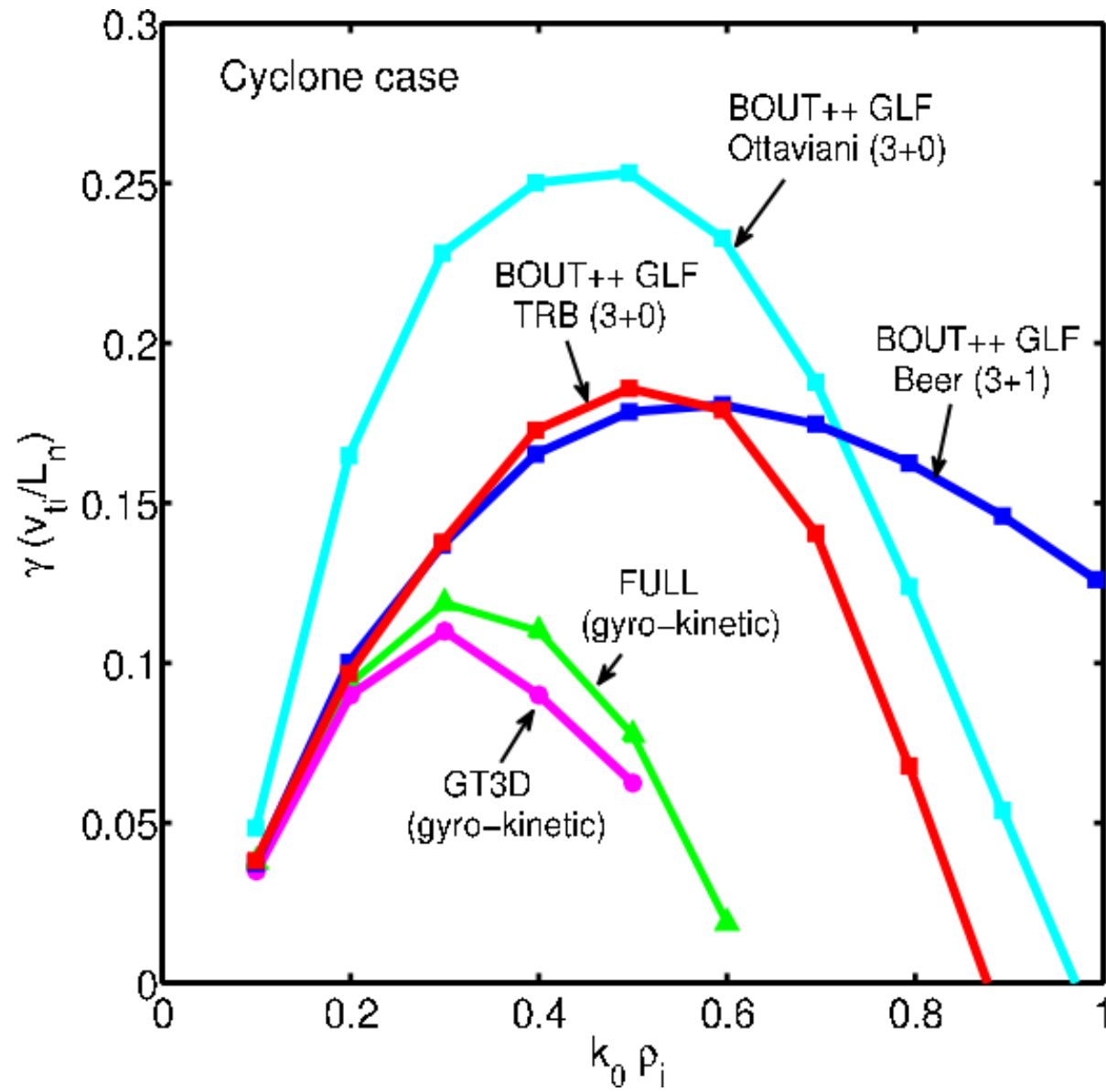
In order to verify the BOUT++ GLF results, Korean GLF Team member, Dr SS Kim, developed a gyro-fluid non-local eigen-value solver to solve the same exact set of equations as in BOUT++ framework.